

Syntheses, characterization, and hydrolytic degradation of P(ϵ -caprolactone-co- δ -valerolactone) copolymers: Influence of molecular weight

Marion Lorient, Isabelle Linossier, Karine Vallée-Réhel, Fabienne Fay

Laboratoire De Biotechnologie Et Chimie Marines EA 3884, Université De Bretagne-Sud, Lorient Cedex BP92116, 56321, France

Correspondence to: F. Fay (E-mail: fabienne.fay@univ-ubs.fr)

ABSTRACT: Biodegradable poly(ϵ -caprolactone-co- δ -valerolactone) copolymers were synthesized and investigated to study their behavior in aqueous medium. The copolyesters were produced by ring opening polymerization between ϵ -caprolactone (CL) and δ -valerolactone (VL) in bulk at 140°C using tin(II) octoate as catalyst. They were characterized by using ^1H NMR, size exclusion chromatography, differential scanning calorimetry, and MALDI TOF mass spectrometry. Reactivity ratio determination gave an insight on their microstructure. Hydration, hydrolytic degradation, and biocide release of P(CL-VL) films with different molecular weights values were studied. A one-order kinetic whose rate constant decreases with copolymer macromolecular weight was observed. Although the molecular weight decrease remained relatively weak after 8 months of immersion, a correlation between molecular weight and hydrolysis rate was shown by high performance liquid chromatography-mass spectrometry. The ability of the P(CL-VL) films to release active compounds dispersed in the films was studied by atomic absorption spectroscopy. The release behavior of all copolymers was identical with a zero-order kinetic. © 2015 Wiley Periodicals, Inc. *J. Appl. Polym. Sci.* **2016**, *133*, 43007.

KEYWORDS: biodegradable; microscopy; properties and characterization

Received 5 June 2015; accepted 2 October 2015

DOI: 10.1002/app.43007

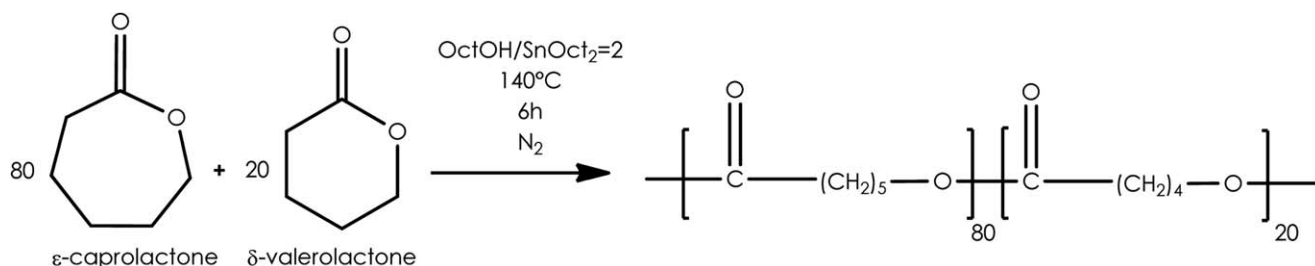
INTRODUCTION

The degradation mechanism of polyesters has been drawing much attention because an important attribute of these polymers is the possibility to modulate their degradation rate.^{1,2} Several delivery systems have been developed by changing their chemical composition (homo or copolymers) or their physical properties (molecular weight, glass-transition temperature).^{3–7} Consequently the drug release can be controlled.^{3,7}

Poly(caprolactone) (PCL) is an important member of the aliphatic polyester family and presents an interest for biomedical applications owing to its good biocompatibility and low immunogenicity. For molecule release applications, the advantages of PCL include its high permeability to drugs and poor water swelling capacity.³ PCL has been exploited for the development of tissue engineering scaffolds and controlled release systems.^{6–8} Its compatibility with a wide range of drugs enables uniform drug distribution in the formulation matrix and its long-term degradation facilitates drug release up to several months.⁷ Nevertheless, applications of PCL remain limited because its degradation kinetics is considerably slower than other aliphatic polyesters (2–4 years). This is due to its hydrophobic character

and its high crystallinity.⁸ A huge resurgence of interest during the 1990s and 2000s has propelled PCL back into the biomaterials. Introduction of functional groups into PCL,^{9–11} irradiation of doped PCL films,¹² blends of copolymers,¹³ or copolymerization with co-monomers with different architectures^{3–5} provide different strategies to tailor the PCL film properties thereby widening the range of their possible applications.⁸ It has been observed that co-polymerization alters the chemical property that indirectly affects all others properties such as crystallinity, solubility, and degradation pattern resulting in a modified polymer with expanded properties for drug delivery.^{7,14}

Our previous works have shown that the incorporation of δ -valerolactone (VL) led to a faster degradation than PCL homopolymer.^{15,16} In this work, to understand the water diffusion effect on the degradation and release mechanisms, we performed a comparative study of P(CL-VL) copolymers with different molecular weights. We synthesized P(CL-VL) by ring opening polymerization of CL and VL promoted by octanol and Tin(II) octoate. As catalyst, SnO_2 allows the production of polyesters with a good control in terms of molecular weight, composition, and microstructure.⁸ By using the characterization methods differential scanning calorimetry (DSC) and MALDI-



Scheme 1. Synthesis of copolymers by ring opening polymerization.

TOF, the crystallinity and structure of the copolymers were studied. Hydration was followed by Karl–Fisher titration and confocal laser scanning microscopy (CLSM). Degradation was studied by size exclusion chromatography (SEC) and high performance liquid chromatography–mass spectrometry (HPLC–MS). Active molecules release was evaluated by atomic absorption spectroscopy (AAS).

EXPERIMENTAL

Materials

ϵ -Caprolactone (CL, Aldrich), δ -valerolactone (Acros), and tin(II) octoate (98%, Aldrich) were used as received without further purification. Octanol was purchased from Aldrich, tetrahydrofuran (THF), petroleum ether from Fisher. Zinc pyriothione (ZnPT) was furnished by Nautix Company.

Copolymerization

P(CL-VL) copolyesters (~20 g) were synthesized in bulk by ring opening polymerization of CL and VL under nitrogen atmosphere. Octanol and tin(II)octoate were used to promote copolymerization with an initial molar [octanol]/[SnOct₂] ratio of two upon a coordination–insertion mechanism (Scheme 1).¹⁷ A reaction time of 6 h was sufficient to reach the conversion of both monomers. The DP_n molar ratio varied from 45 to 180. After degassing at 140°C (10 min) to avoid the presence of humidity, the reaction was carried out for 6 h at 140°C, and the reaction was terminated by quenching in an ice bath. A mechanical agitation was performed to homogenize the mixture. The polymers were recovered by the dissolution/precipitation method with THF as solvent and petroleum ether as no solvent. Polymers were recovered by filtration and drying at room temperature (20°C).

Reactivity Ratio

Series of copolymerizations was carried out at 140°C for periods of 4 min with catalyst concentrations as described above. The reactions were stopped by quenching in ice for obtain 10% conversion. This rate is required in order to calculate reactivity ratios and obtain relative reactivities. Copolymers compositions and percent of conversion were obtained from the pre-purified polymers by ¹H NMR.

Preparation of the Varnishes

To evaluate the capacity of the copolyesters for hydrolysis, films were prepared from a solution containing equal weights of copolymer and xylene. A layer of coating was deposited with an automatic film applicator (ASTM D823 Sheen instrument) on a polycarbonate support. The specimens were dried at 20°C until they achieved a constant weight (dried thickness: 80 μm aver-

age). For active molecules release study, 10% (w/w) of zinc pyriothione was added.

Hydration Kinetics

Films of 1 cm diameter were cut off in order to quantify water amount present in the film. The films were immersed into demineralized water at 20°C. At each sample times, surrounding water was changed to avoid the development of microorganisms. The films were analyzed by Karl–Fisher titration.

Hydration Observation

Films were prepared by adding Nile Red (21 mg/L) in solution containing equal weights of copolymer and xylene. Pieces of films (2 × 3 cm) were immersed in fluoresceine solution (37 mg/L). The films were observed by CLSM.

Hydrolytic Degradation

At each degradation time, three replicates of each specimen were withdrawn from the degradation medium (demineralized water at 20°C), dried, and analyzed by SEC. The appearance of hydroxycaproic acid and hydroxypentanoic acid in aqueous medium was monitored by HPLC–MS in triplicate.

Characterization Techniques

Molecular Weight Measurements. Average molecular weights were determined by Gel Permeation Chromatography (GPC) using a Merck pump L-7110 with two columns PLgel (mixte C, 3 μm and mixte D, 5 μm , from polymer laboratories) in series, and a Sedex DEDL detector (55°C, 2 mbar). THF was used as eluent at a flow rate of 1.0 mL/min and the injection volume was 20 μL . A calibration curve was generated with polystyrene standards (Easical PS-2) purchased from Agilent Technologies. Samples concentration was 1 mg/mL. Data were analyzed by Cirrus software.

Thermal Analysis. Thermal analysis was conducted by DSC using a Mettler-Toledo DSC 822 (Mettler Toledo, Viroflay, France). The samples were scanned from 25°C to 80°C at a heating rate of 20°C/min then cooling at –100°C at 3°C/min, and scanned again from –100°C to 80°C at a heating rate of 3°C/min. The glass transition temperature (T_g) was taken as the midpoint of the transition. The melting temperature (T_m) was taken as the summit of melting peak and ΔH_m was calculated from the area of the endothermic peak after the second run.¹⁶ The degree of crystallinity for a copolymer AB is defined as

$$X_c(\text{AB}) = \frac{\Delta H_m(\text{AB})}{\Delta H_m^0(\text{A})} \omega_A + \frac{\Delta H_m(\text{AB})}{\Delta H_m^0(\text{B})} \omega_B \quad (1)$$

where X_c is the weight fraction of crystallinity, ΔH_m is the enthalpy of fusion measured at the melting point, ΔH_m^0 is the

Table I. Characteristics of P(CL-VL) Copolymers

Copolymers	Rate CL/VL (¹ H NMR CDCl ₃)	Theoretical mass ^a (g/mol)	M _n ^b (g/mol eq PS in THF)	M _n ^c (g/mol)	M _n ^d	PDI	Yield (%)
P12	82/18	5000	12 000	6200	7000	1.7	95
P25	82/18	10000	25 000	13500	14500	1.5	90
P40	83/17	20000	40 000	22500	23200	1.3	89

^aM_n = [monomer]/[SnOct₂] × M₀; M₀ = 111 g/mol.

^bDetermined by SEC, calibration linear polystyrene standard (THF solvent).

^cCorrected value for PCL using M_n(PCL) = 0.259M_n(PS)^{1.073} (Ref. 18).

^dDetermined by SEC, calibration MALDI-TOF (correcting factor 0.58) (Ref. 16).

enthalpy of fusion of the totally crystalline polymer, ω is the weight fraction of each comonomer in the copolymer.

Nuclear Magnetic Resonance Spectroscopy. The 500 MHz ¹H NMR spectra of the samples were recorded at room temperature in CDCl₃ on a 500 Bruker spectrometer.

¹H NMR (500 MHz, CDCl₃, δ): 4.05 (4H, VL5, VL6), 2.3 (2H, CL2, VL2), 1.65 (8H, CL3, CL5, VL3, VL4), 1.35 (2H, CL4); ¹³C NMR (200 MHz, CDCl₃, δ): 21 (VL3), 24 (CL4), 26 (CL3), 28 (CL5), 29 (VL4), 34 (CL2), 35 (VL2), 64 (VL5), 65 (CL6), 172 (VL1), 173 (CL1).

MALDI-TOF Mass Spectrometry. MALDI-TOF mass spectrometry was performed using a microflex Bruker Daltonics. Spectra were recorded in a reflector delayed extraction mode at an acceleration voltage of 20 kV. The matrix, α -cyano-4-hydroxycinnamic acid, was dissolved in THF (14 g/L). About 10 μ L of the polymer fractions (collected after SEC separation) were mixed with 10 μ L of the matrix solution. About 1 μ L of the final solution was deposited onto the stainless steel sample slide and allowed to dry in air at room temperature.

Karl-Fisher Titration. Pieces of films (1 cm diameter) were cut off in order to quantify water amount present in the film by Karl-Fisher titration. A coulometer Metrohm KF 831 equipped with a Metrohm 860KF Thermoprep ($T = 150^\circ\text{C}$) was used under an air flow at 80 mL/min. The reactant was Hydranal-Coulomat AG.

Confocal Laser Scanning Microscopy. Images were captured with CLSM using a TCQ-SP2 (Leica Microsystems, Germany). Nile Red ($\lambda_{\text{excitation}}$: 543 nm; $\lambda_{\text{emission}}$: 526–610 nm) and fluoresceine ($\lambda_{\text{excitation}}$: 488 nm; $\lambda_{\text{emission}}$: 500–520 nm) were observed in sequential mode. Optical sections were observed for each 1 μm in the film thickness. Then a reconstruction was carried out by superposition.

HPLC-Electrospray Ionization Mass Spectrometry. The products resulting from the hydrolysis were identified and quantified with an Agilent technologies Series 1100 chromatography comprising a vacuum degasser, a pump, and an autosampler (Hewlett Packard), and a Brüker Esquire-LC mass detector. Twenty microliters of aqueous solution were injected on C18 stationary phase. The quantification was based on peak area measurement. The [M-H]⁻ ions were isolated: m/z are 131, 117 for hydroxycaproic acid and hydroxypentanoic acid monomers respectively, 246 and 217 for dimers, 360 and 317 for trimers and 474 and

417 for tetramers. The solvent consisted in H₂O/CH₃CN 50/50 (v/v) containing 0.04% ammonia. Pentanoic acid was used as internal standard at 50 mg/L.

Atomic Absorption Spectroscopy (AAS). Sampling (100 mL) were acidified with a solution of nitric acid (1%) (1 mL) to dissolve all degradation products. The spectrometer was a SAA Analyst 200 Perkin Elmer. Wavelength used was 213.9 nm. The standard curves were realized with standard from 0.2 to 1 mg/L in nitric acid 1%.

RESULTS AND DISCUSSION

Characterization of Copolymers

Synthesis. Table I shows the results of the bulk copolymerization with three different feed ratios of monomers. The resulting copolyesters were recovered at high yields (up to 89%).

The molar fraction of monomers in the copolymers was determined by ¹H NMR spectroscopy (results obtained earlier¹⁶). The results from ¹H NMR showed that comonomer ratios in copolymer were in good agreement with the feed ratios. Size exclusion chromatograms of copolymers exhibited monomodal molecular mass distribution (Figure 1). The molecular weight (M_n) of the copolymers synthesized ranged from 12,000 to 40,000 g/mol (equivalent polystyrene) with a polydispersity between 1.3 and 1.7.

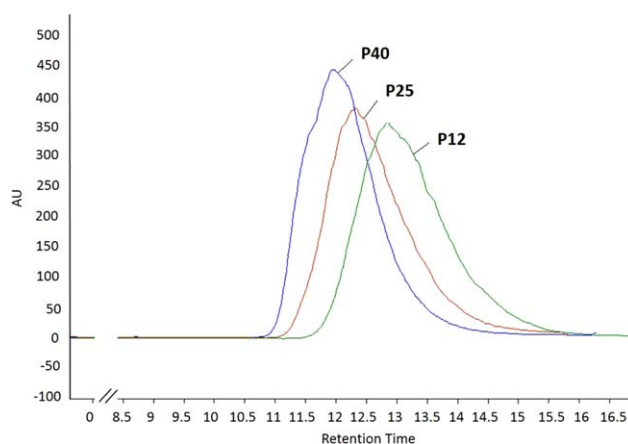
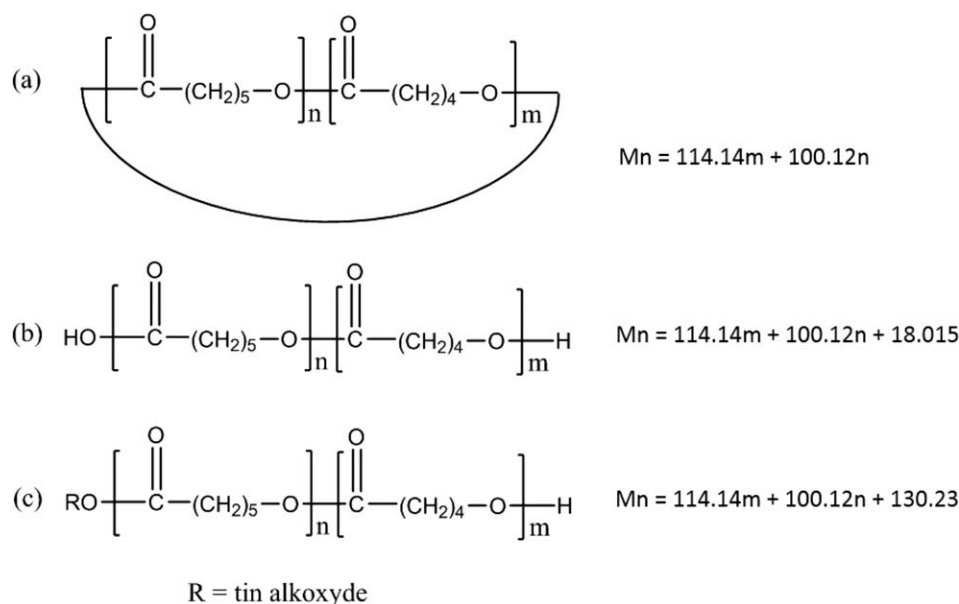


Figure 1. Size exclusion chromatography of copolyesters. [Color figure can be viewed in the online issue, which is available at wileyonlinelibrary.com.]



Scheme 2. Proposed structures of P(CL-VL) prepared by ring opening polymerization.

It is known that direct calibration of SEC measurements with polystyrene calibration overestimates the actual molecular weights of aliphatic polyesters by 50%–80%.¹⁹ For example, Dubois *et al.*¹⁹ proposed an empirical relation to determine an absolute molecular weights for PCL $M_n(\text{PCL}) = 0.259 \times M_n(\text{PS})^{1.073}$. More recently, Hoskins and Grayson²⁰ corroborated these data by SEC analysis coupled with MALDI. Indeed, the MALDI-TOF mass spectrometry is an interesting alternative method.²¹ This technique is particularly interesting when the polymer structure is very different from that of available SEC polymer standards. Moreover, we have previously proposed a corrected factor of 0.58 for P(CL-VL) by using MALDI-TOF MS/SEC offline analysis. As shown in Table I, the results are relatively in good correlation with these previous studies.¹⁶

Structural Analysis. The relatively high polydispersity index could be explained by the polymerization temperature (140°C) and the long reaction-time (6 h) to reach high conversion for

both monomers. As a consequence, transesterification reactions could occur as side-reactions. MALDI-TOF mass spectrometry was used to determine more precisely the microstructure of the copolyesters. Firstly, SEC was performed in THF to obtain fractions with a lower polydispersity ($I_p < 1.2$). Scheme 2 shows the structural assignments of structures of P(CL-VL) that could appear in the MALDI-TOF spectra where N represents the total number of repetitive units, m the number of VL repetitive units and n the number of CL repetitive units. Figure 2 represents the expansion of the region centered between $m/z = 2120$ and $m/z = 2350$ of the MALDI-TOF spectrum. The mass assignments are presented in Table II. Only two types of Na^+ and K^+ -ionized structures (a and c) were detected. These results have confirmed the obtaining of (i) linear structures (structure c, Scheme 2) with a hydroxyl end group at one end and an ester group at the other end and of (ii) a cyclic structure in lower proportion (structure a, Scheme 2).

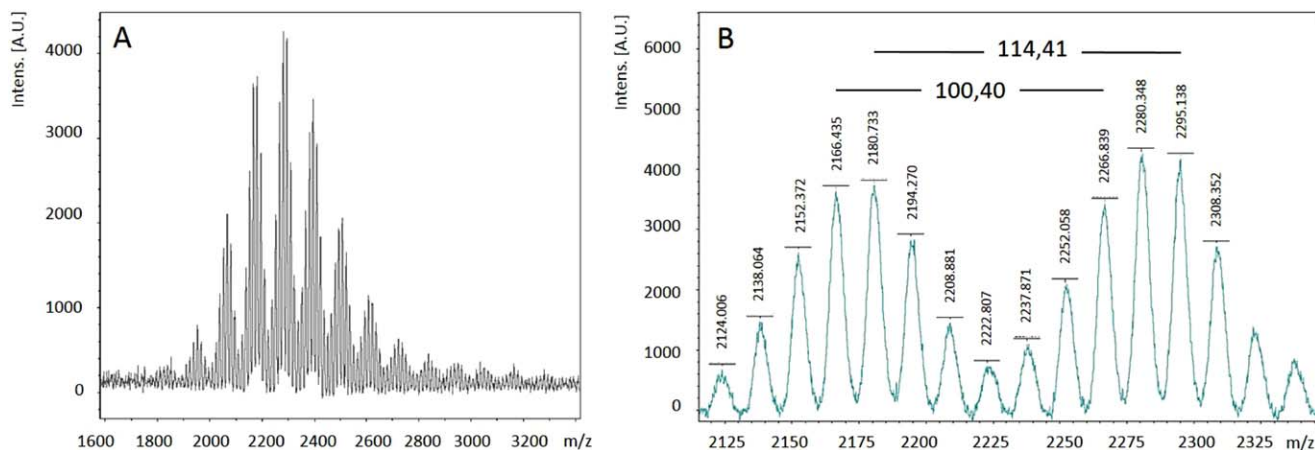


Figure 2. MALDI-TOF mass spectra of P12. [Color figure can be viewed in the online issue, which is available at wileyonlinelibrary.com.]

Table II. Assignment of MALDI ToF Signals

m/z	N ^a	n ^b	m ^b	Ionization	Structure
2138,064	19	14	5	K ⁺	Cyclic
2152,372	18	14	4	Na ⁺	Linear
2166,435	19	16	3	K ⁺	Cyclic
2180,733	18	16	2	Na ⁺	Linear
2194,270	18	17	1	Na ⁺	Linear
2208,881	18	17	1	K ⁺	Linear
2237,871	20	14	6	K ⁺	Cyclic
2252,058	19	14	5	Na ⁺	Linear
2266,839	20	16	4	K ⁺	Cyclic
2280,348	19	16	3	Na ⁺	Linear
2295,138	19	17	2	Na ⁺	Linear
2308,352	19	17	2	K ⁺	Linear

^aTotal number of repetitive units.^bNumber of CL (n) or VL (m) units.

The comonomer sequence is one of the main factors that influence copolymer behavior and properties. The copolymer composition depends on the monomer feed composition and on the relative monomer reactivity. To determine the reactivity ratios of CL and VL, various copolymers were prepared at low conversion (<10%) and their compositions were determined by ¹H NMR spectroscopy. The reactivity ratios were calculated from the composition data by the method of Fineman and Ross²² and Kelen and Tüdös²³ and the values are reported in Table III. The results ($r_{VL} > 1$ and $r_{CL} < 1$), under the reactions conditions, imply that both propagating centers add VL monomers preferentially. The difference in reactivity ratios between VL and CL are slightly higher with $r_{VL}r_{CL} < 1$ indicating that the polymer obtained would possess a slightly blocky structure. Literature data have already reported that the P(CL-VL) copolymers show a tendency for block of the monomer units in the copolymer structure (Table IV). In these different studies, r_{CL} is smaller than 1, and r_{VL} is higher, with $r_{CL}r_{VL} < 1$. However, reactivity ratios were determined at the beginning of the polymerization reaction. Hence, this method ignores the occurrence of secondary reactions as shown above.²⁴ With a 6 h reaction time and a temperature of 140°C, a random microstructure of P(CL-VL) can be considered with micro-domains for copolymer with a high content in one of the comonomer. For example, for P(CL-VL) 82/18 the assumption can be made that long CL sequences with a few VL units are randomly distributed on the macromolecular chains.

Table III. Reactivity Ratios of the δ -Valerolactone and ϵ -Caprolactone during Bulk Copolymerization with Sn(Oct)₂ at 140°C Determined with Kelen and Tüdös and Fineman and Ross Methods

	r_{CL}	r_{VL}	r_1r_{CL}
Kelen Tüdös	0.12	1.21	0.15
Fineman-Ross	0.16	1.18	0.19

Table IV. Reactivity Ratios in Copolymerization of ϵ -Caprolactone and δ -Valerolactone with Different initiators

Initiator	r_{CL}	r_{VL}	$r_{CL}r_{VL}$
Ti(OBu) ₄ (Ref. 16)	0.23	1.93	0.44
SmMe(C ₅ Me ₅) ₂ (Ref. 25)	0.20	2.82	0.56
Diols (Ref. 26)	0.25	0.49	0.12

Characterization of Copolymers by DSC

Glass temperature (T_g), melting temperature (T_m), and crystallinity of copolymers are physical properties which depend on the comonomers composition and distribution and the chain length. DSC was performed to investigate these characteristics. P(CL-VL) copolymers were semi-crystalline: only two peaks were observed corresponding to the glass and melting transitions. These results confirm previous studies.^{16,27,28}

The glass transition temperatures of P(CL-VL) 80:20 were similar regardless of molecular weight. Melting points were lower than PCL homopolymer ones (60°C), reaching a minimum of 33°C. It was possibly due to a rapid decrease of the block length of CL in the copolyester.^{16,27,28} Melting temperature increased slightly with the molecular mass from 33°C to 38°C (standard deviation: 2°C) for molecular weight varying from 12,000 to 40,000 g/mol (PS standard). It is known that melting temperatures increase with molecular weight^{29,30} reflecting a variation in the morphological properties. Indeed, melting enthalpy values (ΔH_m) gave more pronounced results by increasing with molecular weight. The values vary from 60 to 81 J/g. The values of the degree of crystallinity of the samples (X_c) can be calculated from the latent heat of fusion of the copolymers divided by the reported enthalpies of 100% crystalline polymer.³¹ The most commonly used values, considered here for calculations, are close to 136.1 and 181.8 J/g for PCL and PVL, respectively.^{32,33} Table V shows clearly that crystallinity rate increased with molecular weight. It was in close agreement with results published by Odent *et al.*²⁷

Hydration of Copolymers in Varnish

Water uptake, the first phenomenon that occurs when polymeric materials are placed in an aqueous medium, was evaluated by (i) Karl-Fisher titration to quantify the global rate hydration and (ii) CLSM to visualize the hydration zones inside the films.

Before immersion, the films were transparent and colorless. The hydrophobicity can be determined by static contact angle measurement. The three varnishes had the same water contact angle

Table V. Thermal Data Obtained by DSC of the P(CL-VL) (Standard Deviation: 2°C)

Polymer	M_n g/mol eq. PS	T_g (°C)	T_m (°C)	ΔH_m (J/g)	T_c (°C)	Crystallinity X_c (%)
P12	12,000	-71	33	60	13	42
P25	25,000	-68	36	71	14	50
P40	40,000	-67	38	81	15	57

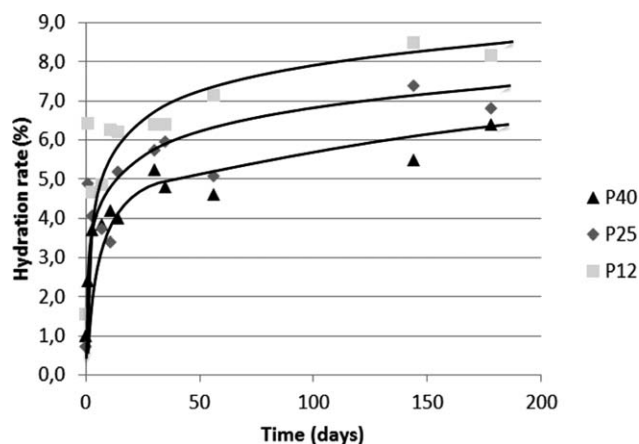


Figure 3. Hydration of varnishes during immersion in demineralized water at 20°C.

$82^\circ \pm 2^\circ$ independently of molecular weight of copolymers. However, after 180 days in the degradation medium, the films became white. The change of color indicates the penetration of water into the films. Water diffusion promoted when the molecular weight decrease.

As shown in Figure 3, the three copolymers had the same pattern of hydration determined by Karl–Fisher titration. A first rapid hydration phase was observed during the first day: the water uptake increased to reach 2.4%, 4.95%, and 6.4% w/w, respectively, for the P12, P25, and P40 films. Then a slower hydration was observed in the second step to reach 13.7%, 10.8%, and 6.9% for P12, P25, and P40, respectively, after 234 days. The hydration of P12 was more pronounced than the two other copolymers. The hydration of films increased as the molecular weight decreased. The result could be explained by the lower crystallinity of the P12 copolymer, so the water can penetrate easily in the polymer matrix.

Simultaneously, CLSM was performed. It enables to visualize the water uptake in the film during the first days of immersion.³⁴ Fluorescein was added to water in order to observe water whereas Nile Red was used to visualize polymer films. Both fluorochromes (fluorescein and Nile Red) possess different excitation–emission properties. Hence, the fluorescence emission can be separated into different channels. The evolution of films during immersion (in blue) was performed (Figure 4). The distribution of the water-soluble fluorescent dye (in pink) in the interior of the polymer films is also visible. The different photographs revealed major differences between the investigated films. P12 was rapidly hydrated in the entire film (after 5 h): an intense pink fluorescence was observed. Inversely, P40 shows a lower hydration with the observation of micro-domains after 24 h. Moreover, homogeneous hydration was observed after a 7 days immersion (Figure 5). Thus, microscopic observations confirm previous observations: the increase of molecular weight decreased the water diffusivity inside P(CL-VL) films. This result can be explained by an increase of the crystallinity.

Degradation of Copolymer in Varnish

Hydrolytic degradation of the films was monitored by SEC and HPLC-MS during immersion. The first method analyzes the molar weight of macromolecular chains whereas the second one quantifies the presence of degradation products in the surrounding water. The different chromatograms obtained by SEC before and after different immersion time did not reveal any significant changes in the molecular weight of P(CL-VL) copolymers. Results were plotted as logarithm of M_n versus degradation time (Figure 6). Very weak changes in M_n were observed for the three P(CL-VL), attesting the very slow degradation of the copolymers. Although, the degradation of copolymers was known to be higher than those of the homopolymers, the P(CL-VL) macromolecular chains seemed to be slightly affected by hydrolysis (down to 5% after 8 months of immersion). Results can be explained by the hydrophobic character of

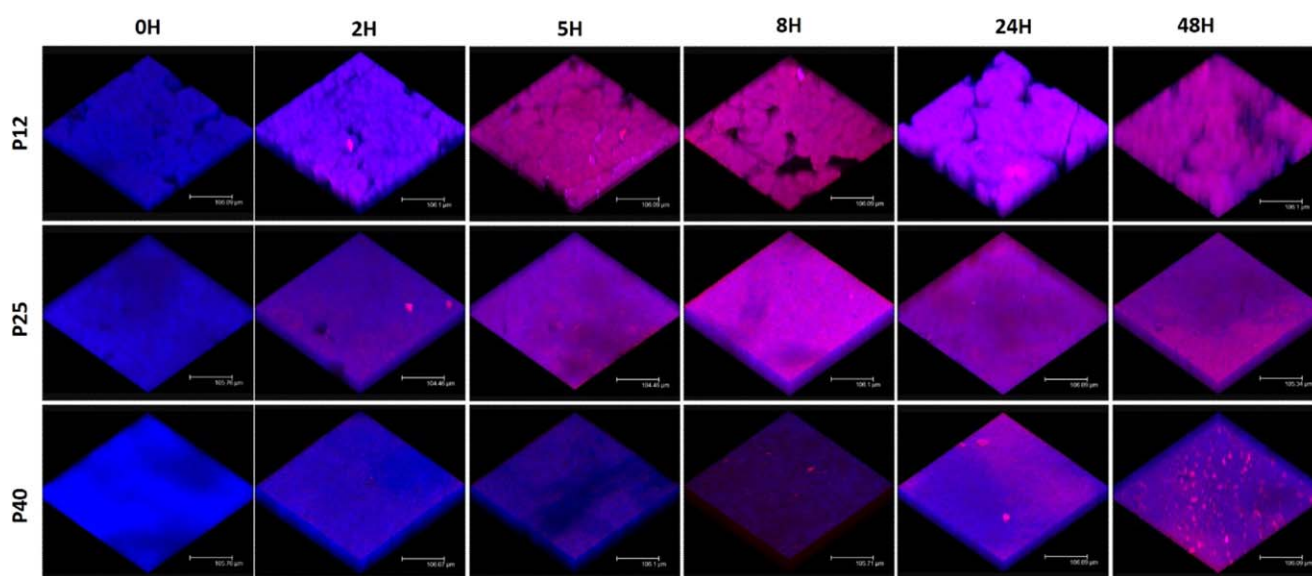


Figure 4. Confocal microscopy three-dimensional renderings of z-stacks of P(CL-VL) films varying with molecular weight during 48 h in aqueous solution of fluorescein (105 μm). [Color figure can be viewed in the online issue, which is available at wileyonlinelibrary.com.]

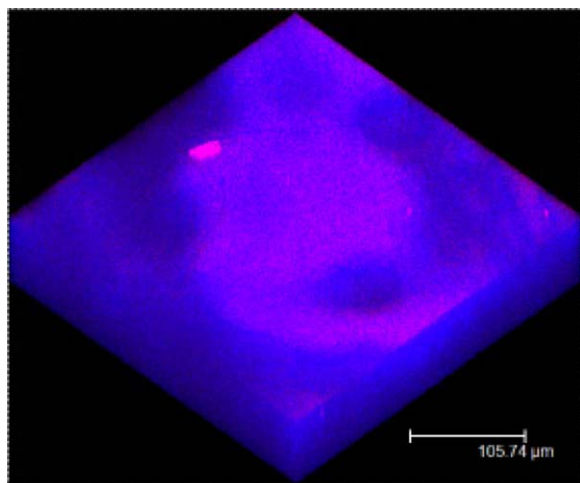


Figure 5. Hydration of P40 after 7 days of immersion (105 μm). [Color figure can be viewed in the online issue, which is available at wileyonlinelibrary.com.]

VL and CL units despite the fact that films were bulk hydrated.³⁵ No influence of molar weight on degradation profile was observed by SEC.

From the well-known exponential relationship between molecular weight and degradation time for biodegradable polyesters in hydrolysis, it is possible to determine the apparent degradation rate (KM_n) and the half degradation time³⁶:

$$\ln M_n = \ln M_{n0} - KM_n t \quad (2)$$

$$\text{and } t_{1/2} = \ln 2 / KM_n \quad (3)$$

where M_n is the average molecular weight, M_{n0} is the initial average molecular weight, KM_n values for P12, P25, and P40 were, respectively, 50.10^{-4} , 56.10^{-4} , and 27.10^{-4} months⁻¹ with corresponding $t_{1/2}$ of 138, 123, and 256 months, respectively. The degradation rate of P40 was the slowest of the films studied, whereas no differences were observed between P25 and P12. Increasing initial molecular weight resulted in an increased molecular weight half-life.³⁷

However, by HPLC-MS, it can be observed the presence of degradation products (hydroxycaproic acid and hydroxypentanoic

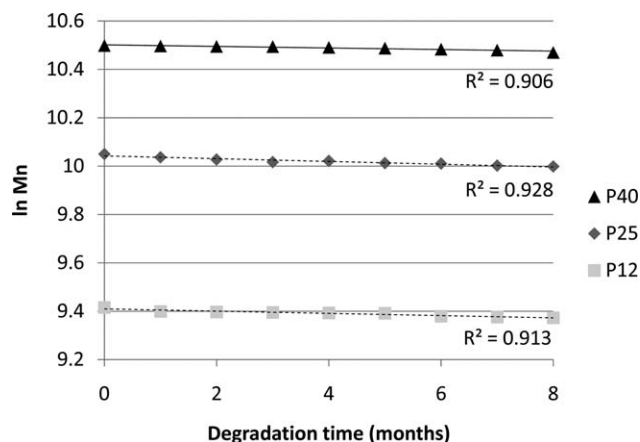


Figure 6. The $\ln M_n$ versus degradation time of the P(CL-VL) copolymers.

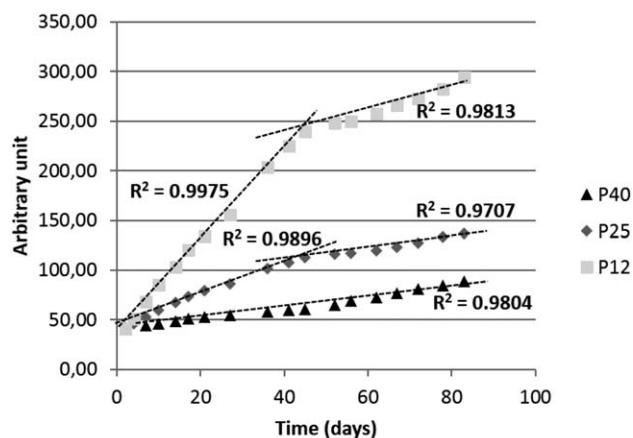


Figure 7. Effect of the molecular weight on the degradation products release.

acid) in the surrounding water. Results are shown in Figure 7. Both degradation products were simultaneously detected because (i) both standards can contain up to 25% average dimers, (ii) electrospray ionization process promotes dimers and trimers formation. Chromatograms show the presence of monomers, dimers and trimers. Hence, the totality of degradation products was quantified (as arbitrary unity) and hydrolytic degradation of the three copolymers was compared.

The hydrolysis mechanisms being considered include random scission, end scission, noncatalytic hydrolysis, and autocatalytic hydrolysis.³⁸ Our results show that P(CL-VL) degradation occurred by end scission because no significant molecular weight reduction was observed whereas degradation products were observed in the surrounding water. The accumulation of oligomers and monomers together is used as an indication for potential mass loss. This assumes that only ester bonds at the end of polymer chains are cleaved. Shih³⁹ suggested that end scission is dominant, at approximately 10 times the rate of random scission.³⁹ Moreover, the contribution of chain-end scission increases with decreasing of the polymer molecular weight since the fraction of chain ends increases as a consequence of the degradation process.⁴⁰

The degradation of copolymer P12, with lower molecular weight occurred faster than that of copolymers P25 and P40. Although a low rate of degradation, the determination of products release in surrounding water by electrospray ionization confirms a decrease of degradation with the molecular weight. Our results confirm that degradation kinetics was highly dependent upon the molecular weight of the polymers.⁶ High molecular weight structures take much longer to degrade, as mediated through the chain length of the polymer. The lower molecular weight film has a higher permeability.

Moreover, different release behaviors were observed. For P40 the amount of degradation products increased linearly with the degradation time, which indicates diffusion at a constant rate. Inversely, P12 and P25 show two steps of diffusion. After 40 days, it is possible to observe a decrease of the release slope. This indicates a modification of diffusion. It is correlated with the hydration profiles of films.

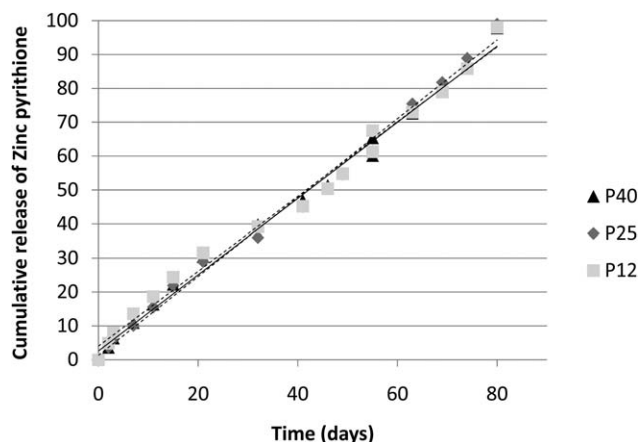


Figure 8. Effect of the molecular weight on the release of zinc pyrithione.

In Vitro Release of Bioactive Molecules

As already seen, the variation of the molecular weight is one of the factors influencing the diffusivity of water and degradation products in the polymer films. These two parameters were known to control the release of bioactive molecules.^{5,41} Therefore, zinc pyrithione (ZnPT), which has good antifouling properties, was chosen as a model biocide.⁴² It is weakly water soluble (15–20 ppm), highly stable and lipophilic (octanol–water partition coefficient = 0.9).⁴²

Films were prepared from varnishes containing (by weight) 40% of copolymer, 10% of ZnPT, and 50% of xylene. The rate of zinc measured by atomic absorption spectrometry in water increased linearly with time whatever the molecular weight (Figure 8). Although P12 had the fastest hydration rate, the biocide release was not the fastest. Lei *et al.*⁴³ have previously found that the molecular weight of PCL had no significant influence on the drug permeation rate of the film. This indicates that the release of this biocide was not correlated with the hydration and degradation of copolymers. Thus, the rate of biocide release was not controlled by the molecular weight of copolymers.

It can be observed that a zero order molecule release behavior for the three films ($M_t/M_\infty = kt$ where M_t and M_∞ are the cumulative amounts of molecule released at time t and infinite time) with the correlation coefficient above 0.99. The zinc concentrations quantified in the surrounding waters never reached the limit of ZnPT solubility. It is known, that degradation mechanism of the polymer in any formulations may indirectly alter the release profile of incorporated active molecules.⁵ SEC results showed that copolymers molecular weights in the films decreased by about 3%–5% after the release test. Considering that the films were substantially stable during the molecule release, it could be assumed that the release is dominated by a diffusion mechanism. This result could be due to a porous structure of films that allows water to diffuse and dissolve the molecules, which complemented the reduction of osmotic pressure of molecule core during release process and maintained molecule constant release.⁴¹ This result was already published by Jones *et al.*⁴⁴ The authors showed that diffusion-controlled release of rifampicin inside polyethylene glycol-poly(ϵ -caprolactone) networks was unaffected by polymer degradation. The

same result was observed by Tarvainen⁷ for PCL films: the degradation rates of the films did not control the release of the drugs and diffusion coefficients of the drugs in the films remained constant.

Moreover, the totality of ZnPT was released after 80 days of immersion. The release depends on the property of active molecules that in turn affects the distribution pattern in PCL formulation.⁵ The lipophilic active molecules are generally distributed uniformly in the matrix while the hydrophilic drugs tend to move toward the interface and remain on the surface of PCL formulation in adsorbed state.⁴⁵ Diffusion is the only possible mechanism by which the lipophilic drugs release from PCL formulation.⁵

CONCLUSIONS

P(CL-VL) copolymers have been synthesized by ring opening polymerization in bulk at 140°C using SnOct₂/octanol as catalyst. This catalytic system leads to the formation of random copolyesters varying with their molecular weight and hence with crystallinity. This result was confirmed by MALDI-TOF analysis and reactivity ratios determination. This parameter affects mainly hydration of copolyester films, and to a lesser extent their hydrolytic degradation. Observations by CLSM proved a homogeneous hydration of films and the kinetics varying with molecular weight. Active molecule release was not affected by the molecular weight and so the crystallinity showing a predominant diffusion mechanism. Hence, by copolymerization with δ -valerolactone, application of PCL can be improved. Copolyesters appear to be very promising for their application in controlled release films.

ACKNOWLEDGMENTS

Nautix Company and the Brittany region in France are fully acknowledged for financial support for this study.

REFERENCES

- Hutmacher, D. W. *J. Biomater. Sci. Polym. Ed.* **2001**, *12*, 107.
- Hofmann, D.; Entrialgo-castano, M.; Kratz, K.; Lendlein, A. *Adv. Mater.* **2009**, *21*, 3237.
- Lu, F.; Shen, Y. Y.; Shen, Y. Q.; Hou, J. W.; Wang, Z. M.; Guo, S. R. *Int. J. Pharm.* **2012**, *434*, 161.
- Ning, Z.; Jiang, N.; Gan, Z. *Polym. Degrad. Stab.* **2014**, *107*, 120.
- Larranga, A.; Aldazabal, P.; Martin, F. J.; Sarasua, J. R. *Polym. Degrad. Stab.* **2014**, *110*, 121.
- Seyednejad, H.; Ghassemi, A. M.; van Nostrum, C. F.; Vermonden, T.; Hennink, W. E. *J. Control. Release* **2011**, *152*, 168.
- Dash, T. K.; Konkimalla, V. *J. Control. Release* **2012**, *158*, 15.
- Woodruff, M. A.; Hutmacher, D. W. *Prog. Polym. Sci.* **2010**, *35*, 1217.
- Tarvainen, T.; Karjalainen, T.; Malin, M.; Peräkorpä, K.; Tuominen, J.; Seppälä, J.; Järvinen, K. *Eur. J. Pharm. Sci.* **2002**, *16*, 323.

10. Jérôme, C.; Lecompte, P. *Adv. Drug Deliv. Rev.* **2008**, *60*, 1056.
11. Jiang, T.; He, F.; Zhuo, R. X. *Polym. Degrad. Stab.* **2013**, *98*, 325.
12. Kosa, C.; Sedlacik, M.; Fiedlerova, A.; Chmela, S.; Borska, K.; Mosnacek, J. *Eur. Polym. J.* **2015**, *68*, 601.
13. Lopez-Rodriguez, N.; Lopez-Arraiza, A.; Meaurio, E.; Sarasua, J. R. *Polym. Eng. Sci.* **2006**, *46*, 1299.
14. Lu, F.; Lei, L.; Shen, Y. Y.; Hou, J. W.; Chen, W. L.; Li, Y. G.; Guo, S. R. *Int. J. Pharm.* **2011**, *419*, 77.
15. Faÿ, F.; Linossier, I.; Langlois, V.; Renard, E.; Vallée-Réhel, K. *Biomacromolecules* **2006**, *7*, 851.
16. Faÿ, F.; Renard, E.; Langlois, V.; Linossier, I.; Vallée-Réhel, K. *Eur. Polym. J.* **2007**, *43*, 4800.
17. Storey, R. F.; Sherman, J. W. *Macromolecules* **2002**, *35*, 1504.
18. Dubois, P.; Barakat, I.; Jérôme, R.; Teyssie, P. *Macromolecules* **1993**, *23*, 4407.
19. Tillier, D.; Lefebvre, H.; Tessier, M.; Blais, J. C.; Fradet, A. *Macromol. Chem. Phys.* **2004**, *205*, 581.
20. Hoskins, J. N.; Grayson, S. M. *Macromolecules* **2009**, *42*, 6406.
21. Rizzarelli, P.; Carrocio, S. *Anal. Chim. Acta* **2014**, *808*, 18.
22. Kelen, T.; Tüdös, F. *J. Macromol. Sci. Part A: Appl. Pure Chem.* **1975**, *A9*, 1.
23. Fineman, M.; Ross, S. D. *J. Polym. Sci.* **1950**, *2*, 259.
24. Coulembier, O.; Degée, P.; Hedrick, J. L.; Dubois, P. *Prog. Polym. Sci.* **2006**, *31*, 723.
25. Yamashita, M.; Takemoto, Y.; Ihara, E.; Yasuda, H. *Macromolecules* **1996**, *29*, 1798.
26. Storey, R. F.; Herring, K. R.; Hoffman, D. C. *J. Polym. Sci. A: Polym. Chem.* **1991**, *29*, 1759.
27. Odent, J.; Raquez, J. M.; Duquesne, E.; Dubois, P. *Eur. Polym. J.* **2012**, *48*, 331.
28. Imasaka, K.; Nagai, T.; Yoshida, M.; Fukuzaki, H.; Asano, M.; Kumakura, M. *Eur. Polym. J.* **1990**, *26*, 831.
29. Jamshidi, K.; Hyon, S. H.; Ikada, Y. *Polymer* **1988**, *29*, 2229.
30. Peponi, L.; Navarro-Baena, I.; Baez, J. E.; Kenny, J. M.; Marcos-Fernandez, A. *Polymer* **2012**, *53*, 4561.
31. Kong, Y.; Hay, J. N. *Polymer* **2002**, *43*, 3873.
32. Avella, M.; Errico, M. E.; Laurienzo, P.; Martuscelli, E.; Raimo, M.; Rimedio, R. *Polymer* **2000**, *41*, 3875.
33. Yevstropov, A. A.; Lebedev, B. V.; Kumagina, T. G.; Lebedev, N. K. *Polym. Sci.* **1982**, 628.
34. Borde, A.; Larsson, M.; Odelberg, Y.; Hagman, J.; Löwenhielm, P.; Larsson, A. *Acta Biomater.* **2012**, *8*, 579.
35. Fernandez, J.; Etxeberria, A.; Sarasua, J. R. *Polym. Degrad. Stab.* **2015**, *112*, 104.
36. Wu, L.; Ding, J. *J. Biomed. Mater. Res.* **2005**, *75A*, 767.
37. Gleadall, A.; Pan, J.; Krufft, M. A.; Kellomäki, M. *Acta Biomater.* **2014**, *10*, 2233.
38. Gleadall, A.; Pan, J.; Krufft, M. A.; Kellomäki, M. *Acta Biomater.* **2014**, *10*, 2223.
39. Shih, C. *J. Control. Release* **1995**, *34*, 9.
40. Fernandez, J.; Larranaga, A.; Etxeberria, A.; Sarasua, J. R. *Polym. Degrad. Stab.* **2013**, *98*, 481.
41. Lin, W. J.; Lee, H. G. *J. Control. Release* **2003**, *89*, 179.
42. Cima, F.; Ballarin, L. *Comp. Biochem. Physiol., Part C* **2015**, *169*, 16.
43. Lei, L.; Liu, X.; Shen, Y. Y.; Liu, J. Y.; Tang, M. F.; Wang, Z. M.; Guo, S. R.; Cheng, L. *Eur. J. Pharm. Biopharm.* **2011**, *78*, 49.
44. Jones, D. S.; McCoy, C. P.; Andrews, G. P. *Chem. Eng. J.* **2011**, *172*, 1088.
45. Wang, X.; Wang, Y.; Wei, K.; Zhao, N.; Zhang, S.; Chen, J. *J. Mater. Process. Technol.* **2009**, *209*, 348.